

Министерство науки и высшего образования Российской Федерации
ФЕДЕРАЛЬНОЕ ГОСУДАРСТВЕННОЕ АВТОНОМНОЕ ОБРАЗОВАТЕЛЬНОЕ
УЧРЕЖДЕНИЕ ВЫСШЕГО ОБРАЗОВАНИЯ
НАЦИОНАЛЬНЫЙ ИССЛЕДОВАТЕЛЬСКИЙ УНИВЕРСИТЕТ ИТМО
ITMO University

ВЫПУСКНАЯ КВАЛИФИКАЦИОННАЯ РАБОТА
GRADUATION THESIS

Система управления силовым преобразователем ветроэнергоустановки,
функционирующей на эффекте Магнуса

Обучающийся / Student Смирнов Данил Алексеевич
Факультет/институт/кластер/ Faculty/Institute/Cluster факультет систем управления и робототехники
Группа/Group R34403
Направление подготовки/ Subject area 13.03.02 Электроэнергетика и электротехника
Образовательная программа / Educational program Цифровые системы управления 2020
Язык реализации ОП / Language of the educational program Русский
Квалификация/ Degree level Бакалавр
Руководитель ВКР/ Thesis supervisor Поляков Николай Александрович, кандидат технических наук, Университет ИТМО, факультет систем управления и робототехники, доцент (квалификационная категория "ординарный доцент")

Обучающийся/Student

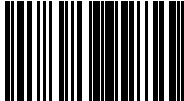
Документ подписан	
Смирнов Данил Алексеевич	
19.05.2024	

(эл. подпись/ signature)

Смирнов Данил
Алексеевич

(Фамилия И.О./ name
and surname)

Руководитель ВКР/
Thesis supervisor

Документ подписан	
Поляков Николай Александрович	
18.05.2024	

(эл. подпись/ signature)

Поляков
Николай
Александрович

(Фамилия И.О./ name
and surname)

**Министерство науки и высшего образования Российской Федерации
ФЕДЕРАЛЬНОЕ ГОСУДАРСТВЕННОЕ АВТОНОМНОЕ ОБРАЗОВАТЕЛЬНОЕ
УЧРЕЖДЕНИЕ ВЫСШЕГО ОБРАЗОВАНИЯ
НАЦИОНАЛЬНЫЙ ИССЛЕДОВАТЕЛЬСКИЙ УНИВЕРСИТЕТ ИТМО
ITMO University**

**ЗАДАНИЕ НА ВЫПУСКНУЮ КВАЛИФИКАЦИОННУЮ РАБОТУ /
OBJECTIVES FOR A GRADUATION THESIS**

Обучающийся / Student Смирнов Данил Алексеевич

Факультет/институт/кластер/ Faculty/Institute/Cluster факультет систем управления и робототехники

Группа/Group R34403

Направление подготовки/ Subject area 13.03.02 Электроэнергетика и электротехника

Образовательная программа / Educational program Цифровые системы управления 2020

Язык реализации ОП / Language of the educational program Русский

Квалификация/ Degree level Бакалавр

Тема ВКР/ Thesis topic Система управления силовым преобразователем ветроэнергоустановки, функционирующей на эффекте Магнуса

Руководитель ВКР/ Thesis supervisor Поляков Николай Александрович, кандидат технических наук, Университет ИТМО, факультет систем управления и робототехники, доцент (квалификационная категория "ординарный доцент")

Характеристика темы ВКР / Description of thesis subject (topic)

Тема в области фундаментальных исследований / Subject of fundamental research: нет / not

Тема в области прикладных исследований / Subject of applied research: да / yes

Основные вопросы, подлежащие разработке / Key issues to be analyzed

Целью данной работы является разработка и исследование системы управления ветроэнергетической установкой на основе эффекта Магнуса для реализации режима работы в рабочей точке с максимальной генерируемой мощностью.

Достижение данной цели требует решения следующего ряда задач:

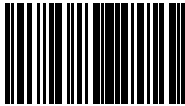
- 1) Разработать имитационную модель системы электропривода вращающихся цилиндров ветроэнергетической установки (ВЭУ).
- 2) Разработать и провести модельное исследование замкнутой системы управления скоростью вращения вращающихся цилиндров ветроколеса ВЭУ.
- 3) Разработать элементы измерительных каскадов устройства управления для реализации алгоритма поиска точки максимальной мощности.
- 4) Разработать реализацию алгоритма поиска точки максимальной мощности для исследуемой ВЭУ и провести его верификацию.

Дата выдачи задания / Assignment issued on: 17.02.2024

Срок представления готовой ВКР / Deadline for final edition of the thesis 30.05.2024

СОГЛАСОВАНО / AGREED:

Руководитель ВКР/
Thesis supervisor

Документ подписан	
Поляков Николай Александрович	
11.05.2024	

(эл. подпись)

Поляков
Николай
Александрович

Задание принял к
исполнению/ Objectives
assumed BY

Документ подписан	
Смирнов Данил Алексеевич	
11.05.2024	

(эл. подпись)

Смирнов Данил
Алексеевич

Руководитель ОП/ Head
of educational program

Документ подписан	
Пыркин Антон Александрович	
17.05.2024	

(эл. подпись)

Пыркин Антон
Александрович

**Министерство науки и высшего образования Российской Федерации
ФЕДЕРАЛЬНОЕ ГОСУДАРСТВЕННОЕ АВТОНОМНОЕ ОБРАЗОВАТЕЛЬНОЕ
УЧРЕЖДЕНИЕ ВЫСШЕГО ОБРАЗОВАНИЯ
НАЦИОНАЛЬНЫЙ ИССЛЕДОВАТЕЛЬСКИЙ УНИВЕРСИТЕТ ИТМО
ITMO University**

**АННОТАЦИЯ
ВЫПУСКНОЙ КВАЛИФИКАЦИОННОЙ РАБОТЫ
SUMMARY OF A GRADUATION THESIS**

Обучающийся / Student Смирнов Данил Алексеевич
Факультет/институт/кластер/ Faculty/Institute/Cluster факультет систем управления и робототехники
Группа/Group R34403
Направление подготовки/ Subject area 13.03.02 Электроэнергетика и электротехника
Образовательная программа / Educational program Цифровые системы управления 2020
Язык реализации ОП / Language of the educational program Русский
Квалификация/ Degree level Бакалавр
Тема ВКР/ Thesis topic Система управления силовым преобразователем ветроэнергоустановки, функционирующей на эффекте Магнуса
Руководитель ВКР/ Thesis supervisor Поляков Николай Александрович, кандидат технических наук, Университет ИТМО, факультет систем управления и робототехники, доцент (квалификационная категория "ординарный доцент")

**ХАРАКТЕРИСТИКА ВЫПУСКНОЙ КВАЛИФИКАЦИОННОЙ РАБОТЫ
DESCRIPTION OF THE GRADUATION THESIS**

Цель исследования / Research goal

Разработка и исследование системы управления ветроэнергетической установкой на основе эффекта Магнуса для реализации режима работы в рабочей точке с максимальной генерируемой мощностью

Задачи, решаемые в ВКР / Research tasks

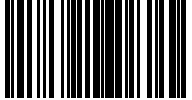
1) Разработать имитационную модель системы электропривода вращающихся цилиндров ветроэнергетической установки. 2) Разработать и провести модельное исследование замкнутой системы управления скоростью вращения вращающихся цилиндров ветроколеса ветроэнергетической установки. 3) Разработать элементы измерительных каскадов устройства управления для реализации алгоритма поиска точки максимальной мощности. 4) Разработать реализацию алгоритма поиска точки максимальной мощности для исследуемой ветроэнергетической установки и провести его верификацию.

Краткая характеристика полученных результатов / Short summary of results/findings

В данной работе при проектировании системы управления ветроэнергетической установкой на основе эффекта Магнуса для реализации режима работы в рабочей точке с максимальной генерируемой мощностью была разработана аппаратная часть обратной связи контура скорости вращающихся цилиндров ветроэнергетической установки, а также система датчиков напряжения и тока, которые необходимы для измерения мощности потребления собственных нужд и вырабатываемой мощности ветроэнергетической установки. На основе экспериментальных данных была разработана модель

электропривода вращающихся цилиндров ветроэнергетической установки и была построена модель регулятора скорости вращения цилиндров. Разработан алгоритм поиска точки максимальной мощности, учитывающий мощность потребления собственных нужд ветроэнергетической установки и формирующий задание по скорости для вращающихся цилиндров. Разработанная система управления реализована в опытном образце и проведены модельные и экспериментальные исследования, подтверждающие ее работоспособность.

Обучающийся/Student


Документ подписан	
Смирнов Данил Алексеевич	
19.05.2024	

(эл. подпись/ signature)

Смирнов Данил
Алексеевич

(Фамилия И.О./ name
and surname)

Руководитель ВКР/
Thesis supervisor

Документ подписан	
Поляков Николай Александрович	
18.05.2024	

(эл. подпись/ signature)

Поляков
Николай
Александрович

(Фамилия И.О./ name
and surname)

CONTENT

INTRODUCTION	5
1 REVIEW OF EXISTING DEVELOPMENTS	7
2 TECHNICAL DESCRIPTIONS OF THE INSTALLATION	12
2.1 Determination of wind turbine design	12
2.2 System Components Overview	12
3 MATHEMATICAL MODEL OF THE CONTROL SYSTEM	15
3.1 Statement of the control problem	15
3.2 Construction of a mathematical model of the rotation speed controller	16
3.3 Development of the MPPT algorithm	21
4 IMPLEMENTATIONS OF THE CONTROL SYSTEM	23
4.1 Selection of components	23
4.2 Development of a block diagram	26
4.3 Implementation of a cylinder control loop	26
4.4 Board development and installation into the system	28
4.5 Experimental comparison of a real system with a model	29
4.6 Implementation of the wind turbine power control loop	30
4.7 Verification of the algorithm's operation	33
CONCLUSION	37
REFERENCES	39
Appendix A	40
Appendix B	41
Appendix C	42
Appendix D	43
Appendix E	44
Appendix F	45
Appendix G	46
Appendix H	47
Appendix I	50

INTRODUCTION

In the modern world, when the problems of climate change and energy security are becoming more acute, the use of wind power plants is becoming an important element of the energy strategy of many countries. Wind energy is a clean, renewable source of energy that has several advantages over traditional sources. In connection with this, there is increasing interest in new approaches to generating energy from wind. One such approach is based on the use of the Magnus effect, a phenomenon in which the rotation of a cylindrical object in a flow of liquid or gas creates a lifting force. Wind power plants operating based on this principle represent a promising direction in the development of wind energy. They offer several advantages, including increased efficiency at low wind speeds, which expands their range of applications and makes them more accessible for use in a variety of climates. Thanks to their innovative concept, Magnus effect wind turbines can become an important component in ensuring energy security and sustainable development, promoting the diversification of energy sources, and reducing negative environmental impacts.

The primary objective when designing a wind turbine control system is to maximize operating efficiency considering variable environmental conditions, such as wind speed and direction, temperature, and air pressure, as well as electrical loads on the elements of the wind turbine power subsystem. For optimal operation of wind turbines, algorithms for tracking the maximum power point are widely used. The use of OTMM algorithms increases the efficiency and performance of wind turbines, optimizing the use of wind energy and reducing losses due to underuse or overshoot. Such algorithms are a key component of modern wind turbine control systems used in the renewable energy industry to optimize power production.

Design features allow wind turbines based on the Magnus effect to develop flexible control systems that allow the operation of wind turbines to be adapted to changing environmental conditions. The wind turbine control system based on the Magnus effect includes a control loop for the speed of rotation of the cylindrical blades, a power control loop (MPPT) and requires feedback on the speed of rotation of the cylindrical blades and on currents and voltages in the stator phases of the generator and voltage in the DC link of the wind turbine converter.

The purpose of this work is to develop and study a control system for a wind power plant based on the Magnus effect. Achieving this goal requires solving several

problems. At the first stage, it is necessary to develop a simulation model of a wind power plant and select the components necessary for operation. The next step will be to develop and conduct a model study of a closed-loop system for controlling the speed of rotation of the rotating cylinders of the wind wheel. To do this, you need to select speed sensors to receive feedback. After that, it is necessary to develop an OTMM algorithm for the wind turbine under study and verify the algorithm using simulation modeling of the “generator - rectifier device” energy subsystem with a closed-loop control system.

Working conditions: Variable wind speed up to 20 m/s. It is required to design a control system consisting of two circuits: a cylinder control circuit and a wind turbine power control circuit.

Required quality indicators for a rotating blade control system:

- Transient time: 3 s
- Maximum overshoot: 3%

Next, we will consider existing analogues of wind power plants operating on the Magnus effect with similar designs and their technical implementations of operating algorithms to form our own technical solution.

1 REVIEW OF EXISTING DEVELOPMENTS

The technology for using the Magnus effect in wind energy has been studied relatively recently; the first developments and experiments began about two decades ago. The concept of using the rotation of cylindrical bodies in air flow to create energy has been proposed and researched by the scientific community over the past few decades. Therefore, there are a limited number of workable and effective solutions that have the potential to be applied on a large scale.

First example of research is the work of the University of Putra, Malaysia [1]. The research was conducted and published in 2018 on the IOPscience portal. The study involved replacing airfoil-shaped wind turbine blades with rotating cylinder blades known as Magnus wind turbines (MWTs), where they generate lift on a rotating cylinder perpendicular to the incoming wind flow. This development uses a wind power plant with a horizontal axis of rotation. The main difference between a VTM and a wind power plant with aerodynamically shaped blades is in the methods of extracting wind energy. Using rotating cylinder blades, the TMV can harvest wind energy at low wind speeds. In addition, the article describes ways to increase productivity by improving the surface of the rotating cylinder blades, for example, using recesses and fins. It is also proposed to use sandpaper to roughen the surface of the rotating cylinder blades, which can further improve the torque produced by the VTM rotor. The advantages of such a structure include a reduction in environmental hazards and noise levels due to the slow rotation of the rotor.

Based on Bychkov's previous patents [2] using spiral fins, the researchers fabricated a VTM model with 6 spiral fins wound around cylinder blades to find the optimal power output value based on the rotation speed of the cylinder blades and proposed an algorithm to control the speed of the rotating cylinder. Figure 1 shows the model used in the performance optimization experiment with an enlarged rotor hub.

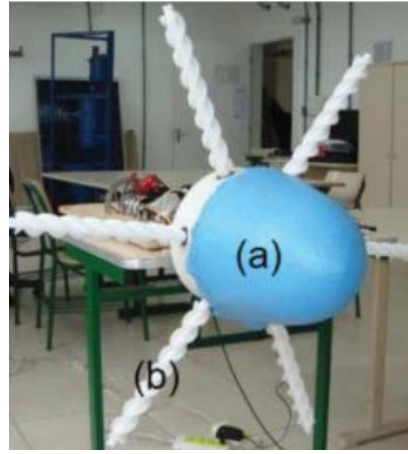


Figure 1 – Experimental model of a wind turbine with spiral fins of blades

Control algorithms in all studies are based on OTMM for wind turbines. The International Journal of Renewable Energy Research papers [3] present an algorithm for a wind power system with a DC servo drive subsystem (DC drive and BLDC motor) to rotate the turbine cylinders. The proposed circuit diagram is shown in Figure 3, the algorithmic diagram for controlling the rotating cylinders is in Figure 4. Optimal rotation of the cylinders is described as providing maximum power extracted from the wind, monitored by a fixed and adaptive HCC (Hill Climbing Control) step acting on the servo. The proposed wind system consists of a PMSG (Permanent Magnet Synchronous Generator), a three-phase diode rectifier, a DC-DC (boost) converter and a resistive load. In addition, the boost converter works with a fixed-step HCC algorithm to track the maximum power operating point. Therefore, OTMM for wind turbines requires monitoring both the optimal cylinder speed and the optimal generator speed.

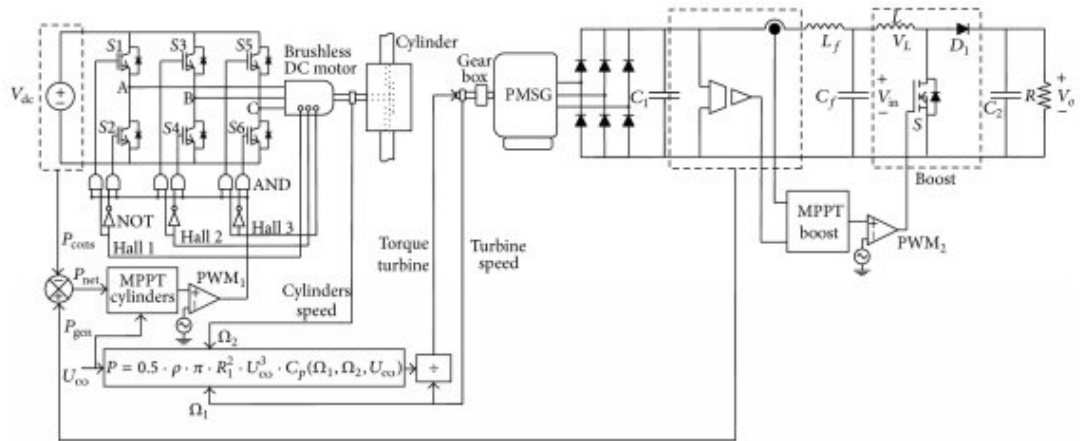


Figure 2 – Schematic diagram of a wind turbine using the Magnus effect

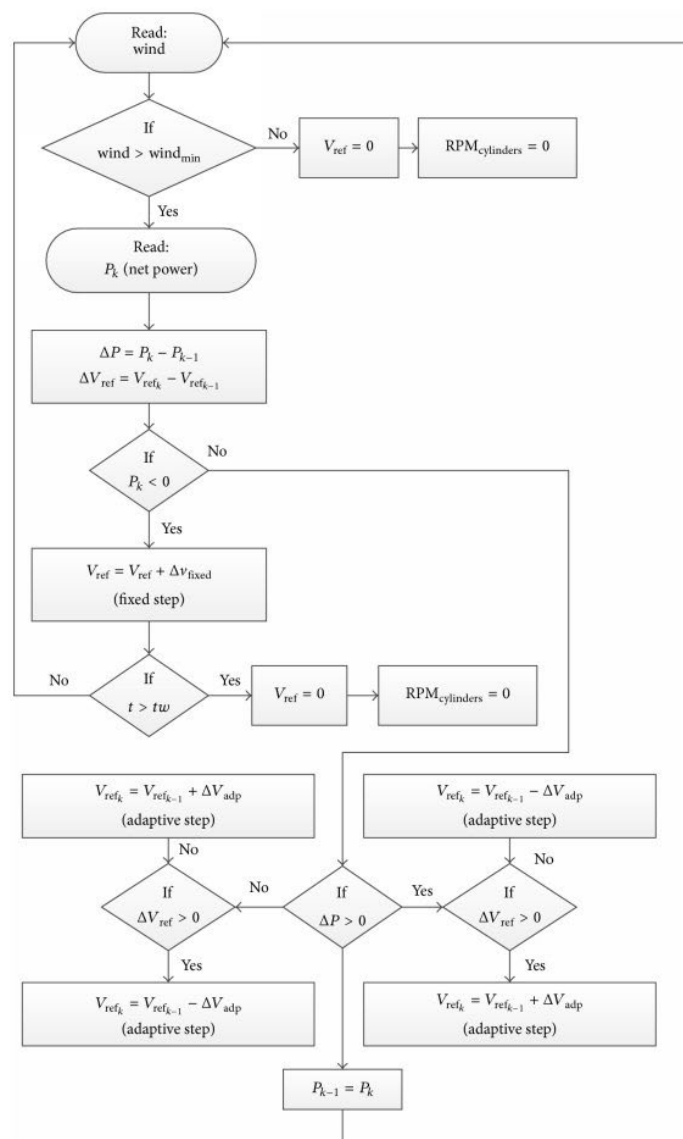


Figure 3 – Algorithmic diagram for controlling rotating cylinders

Another example of development is the work of Turkish researchers from Izmir [4], who created the concept of a wind turbine, which also works on the Magnus effect, on approximately the same principle, but it is proposed to use solar energy in addition to wind energy, by covering the cylinders with solar panels, which should increase energy production. This study builds an analytical framework for the operation of this turbine and makes initial estimates of operating parameters under various conditions and theoretical calculations that can be useful in research and experimentation. In these studies, a control algorithm based on OTMM was also used.

The next development [5] was presented in Japan in 2023 in the city of Okinawa and is currently at the research stage. The main difference is that the installation has a vertical axis of rotation and is powered by energy generated by typhoons, which is relevant for the region. The installation can generate energy at wind speeds of up to 144 km/h, while a conventional propeller-type wind turbine reaches a limit of 90 kilometers per hour. Additionally, the overall rotation speed is much lower than a propeller-type wind turbine, so it reduces noise and bird strikes. Currently, a low-power 10kW pilot model is expected to be installed on isolated islands and remote areas as an independent power source, but a 100kW medium-power model is planned to be launched by 2025 for both offshore and onshore applications, which will act as the main source of energy. In addition, the sample is capable of extracting energy from the decomposition of seawater into hydrogen.

Another development [6], based on research [7] of the Novosibirsk Institute of Theoretical and Applied Mechanics named after S. A. Khristianovich, was presented in Minsk, Belarus. Studies conducted in Minsk and Novosibirsk have shown that under certain conditions (geometry, dimensions, cylinder rotation speed, etc.), the efficiency of using free-stream power at low wind speeds is significantly higher than for conventional bladed wind turbines.

The Aerolla company, together with a team of employees of the National Academy of Sciences of Belarus, created an experimental rotary wind turbine with a capacity of 100 kW, which was installed near the Minsk ring road. The turbine rotor diameter is 36 m, the estimated wind speed is 9.5 m/s. In Novosibirsk, the Institute of Theoretical and Applied Mechanics of the Siberian Branch of the Russian Academy of Sciences, based on fundamental research, has developed a schematic diagram of a new type of high-torque wind turbine (WEM) - with rotating cylinders

and additional improvements. The operating range of wind speeds is at least 2–40 m/s instead of 5–25 m/s for bladed wind turbines. Energy production and daily work duration increase by 2 times or more.

The optimal power range is from 30 to 500 kW, the maximum is up to 2 MW with a wind wheel diameter of 15–50 m or more.

The articles of the Ural Federal University [8] present a study of the installation described above, which talks about the incorrect choice of place for the experiment and the dampness of the invention, but the results are called more than satisfactory. The creators themselves cite the complexity of the design and the high consumption of materials as the main disadvantages.

Based on the results of the review search, it can be concluded that there is a limited number of developments and studies in the public domain that either appeared recently and are in an experimental state or are just planning to launch in the near future, work only under certain climatic conditions and have a limited range of different designs. Existing management systems have already proven their efficiency and have great potential for development. This means that this area is promising for study and experimentation.

Based on the studied implementations, the goal of our own technical implementation was formed, which is to develop and study a control system for a wind power plant based on the Magnus effect to implement the operating mode at the operating point with the maximum generated power. Achieving this goal requires solving the following series of tasks:

- 1) Develop a simulation model of the electric drive system of rotating cylinders of a wind power plant.
- 2) Develop and conduct a model study of a closed-loop system for controlling the speed of rotation of the rotating cylinders of a wind turbine.
- 3) Develop elements of the measuring cascades of the control device to implement the algorithm for searching for the maximum power point.
- 4) Develop an implementation of an algorithm for finding the maximum power point for the wind turbine under study and carry out its verification.

2 TECHNICAL DESCRIPTIONS OF THE INSTALLATION

2.1 Determination of wind turbine design

A wind power plant based on the Magnus effect includes several key components.

The base of the installation is a strong, straight pole that provides a stable position and can withstand gusts of wind. At the top of this pillar there is an engine that operates as a generator, converting the mechanical energy of the wind into electrical energy. A rectifying device is connected to this generator to process the received energy.

An axis on which cylindrical blades are located is attached to the generator rotor. Brushless DC motors are installed inside each blade. They set the cylindrical blades in motion, creating lift due to the Magnus effect, and driving the rotation of the generator rotor. This process allows the installation to generate electricity from wind.

Switched motors, also known as brushless DC motors, have several advantages over traditional DC motors. They are much more compact, have higher efficiency and less energy loss due to the absence of brushes and commutator, making them more energy efficient. Also, due to the absence of brushes, wear and friction inside the motor are significantly reduced, which leads to longer service life and increased operational reliability. But despite all the advantages, such engines require a more complex starting, control and stopping system. Therefore, for the correct operation of switch motors, you need a device that performs all these functions - a driver.

2.2 System Components Overview

To further improve the system and control algorithms, all its component parts were identified. The engines that drive the cylindrical blades are T-Motor MN4014-9 KV400 engines (Figure 4). This is a brushless motor that has been designed for use in multi-rotor applications where high efficiency and reliability are required. It has very low weight, compact dimensions, and a wide range of applications, which is advantageous for use in the developing system.



Figure 4 – T-Motor MN4014-9 KV400 brushless motor

To effectively control the selected motors, the Hobbywing Skywalker HW-BQ800 ESC driver is installed (Figure 5). This device allows you to regulate the engine rotation speed by changing the voltage supplied to it and the frequency of the control signal. It is also equipped with safety mechanisms such as overload, overheating and short circuit protection to ensure the safe operation of the system and prevent damage to components. But for correct operation, a calibration procedure is required before use, during which the minimum and maximum values of the control signal are determined.



Figure 5 – Hobbywing Skywalker HW-BQ800 driver

The power source was a step-down voltage converter RuiDeng RIDEN RD6012 (Figure 6). It plays an important role in the power supply system of the wind turbine motors, as it provides a stable voltage, which avoids overloads and damage to the electronics. This device also provides the ability to regulate the output voltage, which allows you to adjust the power of the installation in accordance with

operating conditions. Equipped with protection mechanisms that prevent damage to the system in the event of overloads or short circuits.



Figure 6 - DC power supply RIDEN RD6012

3 MATHEMATICAL MODEL OF THE CONTROL SYSTEM

3.1 Statement of the control problem

At the time of the start of research, the system in question is controlled by the MyRIO controller, which sends a command signal for the speed of rotation of the blades directly to the engine drivers and does not receive feedback. Thus, the system is open-loop. Open-loop control is not an effective solution for energy synthesis for a variety of reasons. The main one is the lack of error correction. This means that the system cannot compensate for changes in input parameters or external conditions such as wind speed and direction. Without feedback, the system is unable to maintain the set speed, which can result in under or over generation of power. Also, the presence of speed feedback will be useful for diagnosing errors and malfunctions in the system. Therefore, for efficient operation it is necessary to build a controller for a closed system with speed feedback.

To synthesize a regulator, it is necessary to formulate qualitative requirements for a regulator of the rotation speed of cylindrical blades. Since the system was originally developed to generate energy in regions with low wind speed and variability, minimizing the transition process time is not necessary and a few seconds will be enough to achieve the given speed. At the same time, the presence of large overshoot in the system will indicate ineffective energy consumption. Therefore, the requirements can be expressed numerically:

- Transition time – no more than 3 seconds,
- Overshoot – 3%

As for the reference signal, it is first necessary to carry out an experiment with the motor to measure the maximum and minimum rotation speed and the corresponding voltages that will be supplied to the motor driver.

The next task will be to develop an OTMM algorithm that will search for the point at which the device will produce the maximum amount of energy at the current wind speed. The algorithm will send this wind speed to the first control loop in the form of a reference signal.

3.2 Construction of a mathematical model of the rotation speed controller

To control the speed of a brushless DC motor, an effective solution is to use a proportional integral (PI) controller. A PI controller is a type of control device that has two main components: proportional and integral parts.

The proportional part of the controller provides control in accordance with the current error between the setpoint and the actual speed value. The greater the error, the greater the control effect of the proportional part. This allows you to quickly respond to changes in speed and achieve the required value.

An integral part of the controller compensates for static control error, which can occur due to various factors such as friction or irregularities in the system. It integrates the error over time and applies a control action that varies in proportion to the accumulated error. This reduces persistent error in the system and allows for more precise speed control.

The advantages of a PI controller include high speed control accuracy, robustness to external disturbances, and ease of parameter tuning. However, for optimal operation of the regulator, it is necessary to correctly select the coefficients of the proportional and integral parts, which may require some experience and testing under specific engine operating conditions. The control signal for the engine is generated by the regulator in the form:

$$u(t) = K_p e(t) + K_i \int_0^t e(t) dt \quad (1.1)$$

With an increase in the proportionality coefficient (K_p), an increase in the speed of reaching the steady-state value and an increase in the control signal are observed. Mathematically, the system is unable to achieve the exact target value because the component decreases proportionally as it approaches installation. An increase in K_p beyond the optimal values leads to a loss of stability of the real system and the occurrence of oscillations.

Increasing the integration coefficient (K_i) leads to faster error compensation over time, which contributes to the accurate output of the system to the set value. However, if the system response is slow and the value of K_i is too large, overshoot may occur, manifested in undamped oscillations with a long period. To prevent this, the integral sum in the controller algorithm is often limited to avoid its endless growth and reduction.

To successfully implement a BLDC control system, it is necessary to carry out two main stages: the first is to develop a mathematical model of the engine, which should adequately reflect its physical characteristics, and the second is to build a speed controller capable of meeting the requirements of the control task.

A three-phase brushless motor can be described by the following system of equations:

$$\begin{aligned} U_a &= R_a i_a + L_a \frac{di_a}{dt} + E_a \\ U_b &= R_b i_b + L_b \frac{di_b}{dt} + E_b \\ U_c &= R_c i_c + L_c \frac{di_c}{dt} + E_c, \end{aligned} \quad (1.2)$$

where R_a, R_b, R_c – resistance in the stator windings, L_a, L_b, L_c – stator winding inductance, E_a, E_b, E_c – rotational back-EMF induced in the stator windings.

The value of the back-EMF of the windings and the angular speed of rotation of the motor are related through the value of its design constant C_e :

$$E_a = C_e \omega \quad (1.3)$$

From here we can express the magnitude of the angular velocity at idle:

$$\omega_{xx} = \frac{E_a}{C_e} \quad (1.4)$$

Newton's second law for rotational motion describes the dynamics of the engine in the form:

$$M_d - M_s - M_{vt} = J_s \frac{d\omega_m}{dt}, \quad (1.5)$$

This means that the speed transfer function can be expressed as:

$$\begin{aligned} M_d - M_s - B\omega &= J_s s \omega \\ M_d - M_s &= (J_s s + B) \omega \\ \omega &= \frac{M_d - M_s}{J_s s + B} \end{aligned} \quad (1.6)$$

where M_d – moment on the shaft, M_s – moment of external forces acting on the engine, M_{vt} – viscous friction moment, J_s – total moment of inertia reduced to the motor shaft.

To conduct experiments, it is necessary to assemble a setup consisting of a test machine, a load machine, and a driver, and then take measurements at several points; the experimental setup is shown in Figure 7.



Figure 7 – Experimental setup for determining parameters

The rotation frequency is measured using a tachometer, the voltage between phases is measured using an oscilloscope, the results are presented in Table 1. The formula for calculating C_e - the constant EMF of the electric motor:

$$C_e = \frac{2E_{ab}}{3\omega} \quad (1.7)$$

Table 1 – Results of the experiment with speed and voltage measurements

ω , rpm	E_{ab} , V	C_e
1208	2,167	0,001196
1645	2,948	0,001195
2299	4,1071	0,001191
2687	4,7895	0,001188
2930	5,2174	0,001187

The next step was to measure the frequency of the reference signal, which the regulator sends to the engine using an NI Elvis III oscilloscope; the experiment graph

is presented in Figure 8. The frequency of the measured signal is 8 kHz.

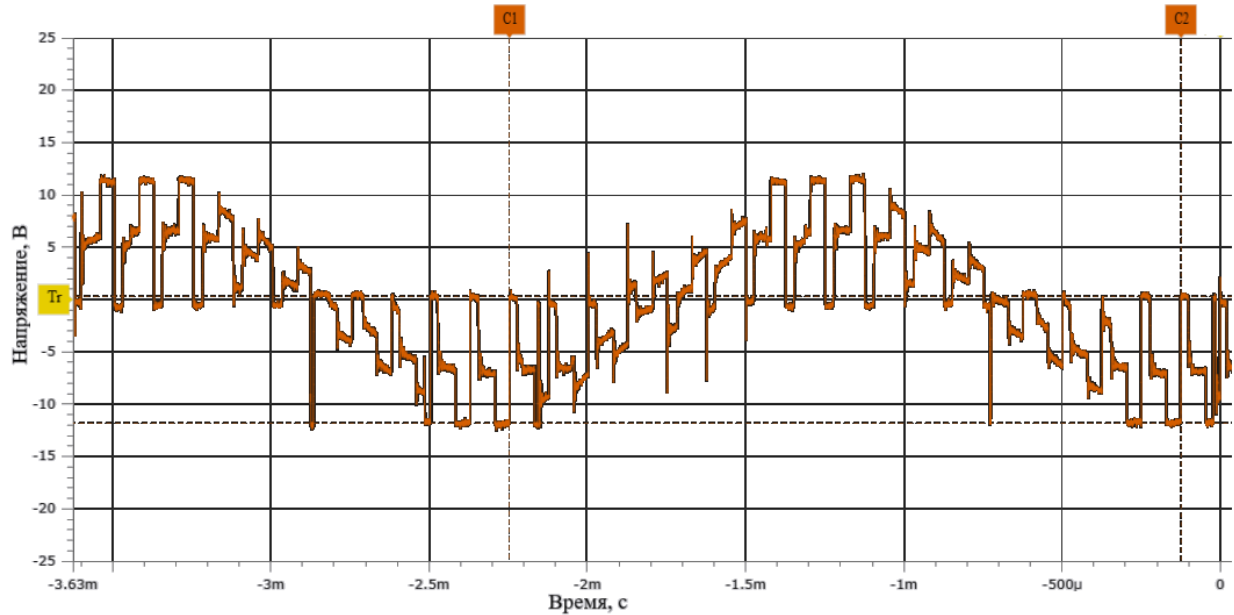


Figure 8 – Oscillogram of the motor control signal

After which the active resistance and inductance were measured at a given frequency, the results are presented in Table 2.

Table 2 - Results of the experiment on measuring resistance and inductance

№ эксперимента	$L_s, \mu\Gamma$	$R, \text{Ом}$
1	37,75	0,2665
2	42,833	0,2999
3	42,687	0,294
4	37,861	0,2669
5	42,809	0,3009

The values of the moment of inertia for the engine, considering cylindrical blades, were taken from the work in which the dynamic characteristics of the present system were studied [9].

Thus, the following parameter values were obtained:

$$C_e = 0,001188$$

$$L_s = 40,788 \mu\text{H}$$

$$R = 0,28 \text{ Ohm}$$

$$J = 3,53 * 10^{-3} \text{ kg} * \text{m}^2$$

The PI controller was tuned using the experimental-analytical method. Initially, only the proportional gain of the controller was selected, which made it possible to achieve a constant error, but the value was close to the target. After which the integral coefficient was substituted, starting with small values, which made it possible to achieve convergence to the true value. The block diagram is shown in Figure 9.

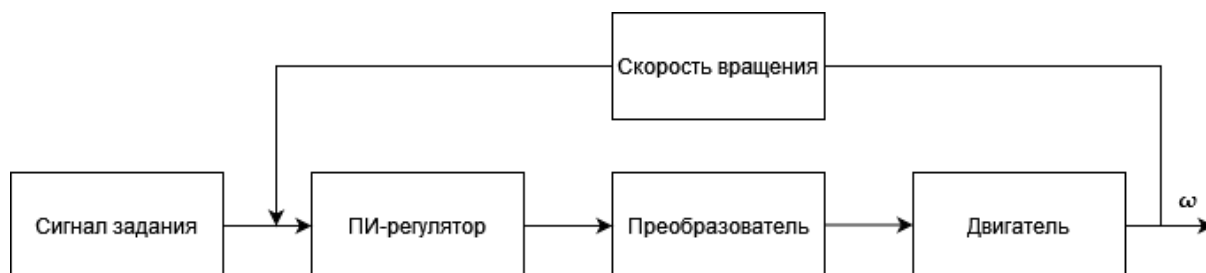


Figure 9 – Block diagram of a closed-loop control system

Simulation was carried out in Matlab/Simulink environment. The diagram is presented in Figure 10, the simulation results are shown in Figure 11.

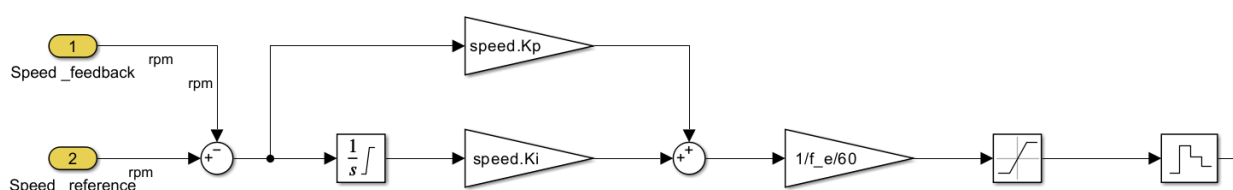


Figure 10 – Model of a closed system in the Matlab/Simulink environment

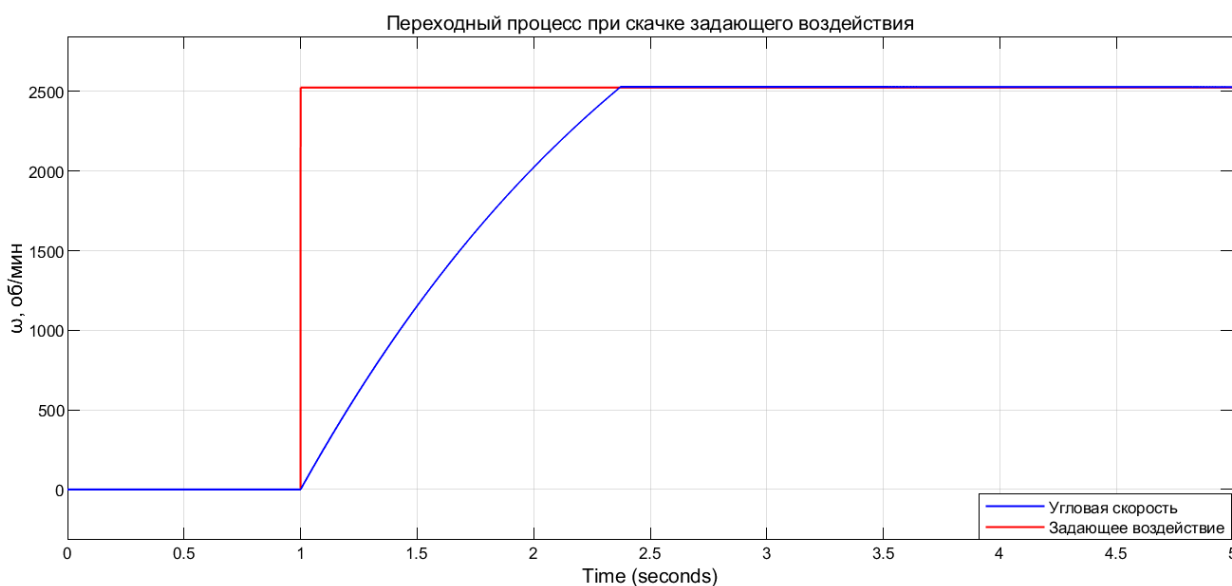


Figure 11 – Simulation results

The parameters of the TPCA8057-H field-effect transistor, on which the ESC motor controller is based, are presented in Appendix B. A model of the complete control system is presented in Figure 12.

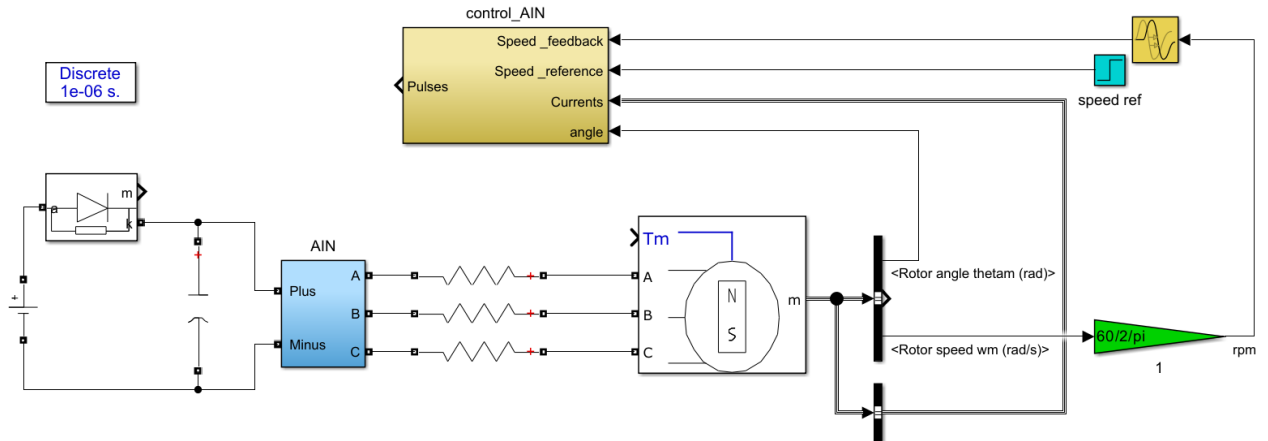


Figure 12 – System model in Simulink environment

3.3 Development of the MPPT algorithm

The next stage is to develop an OTMM algorithm that will generate a command signal for the first control loop in the form of rotation speed of cylindrical blades based on the generated and consumed power.

Maximum power point tracking (MPT) algorithm is a control method used in wind turbine (WPP) systems that aims to maximize power production by optimizing rotor performance under varying wind speed conditions.

The principle of operation of the algorithm is to constantly calculate the optimal rotor speed at which the power generated by the wind turbine reaches its maximum value under current atmospheric conditions. To do this, the algorithm continuously adjusts the rotation speed of the cylindrical blades, that is, sets the optimal speed value for the engines that drive them.

The control system receives information about the current and voltage of the source and generator, calculates the difference between the expended and generated power and finds the maximum power point that corresponds to the optimal operation of the wind turbine. The algorithm is in real time, continuously analyzing changes in wind conditions and adjusting rotor parameters to maintain operation at the maximum power point.

The algorithm itself can be described in the form of a block diagram, which is presented in Figure 13, where P_{MEX} – generating power, ω_1 – cylindrical blade speed,

ω_{step} – speed change step, $\Delta P = P_{mex} - P_{old}$, $\Delta\omega = \omega_1 - \omega_{1old}$, P_{old} – power value at the previous iteration, ω_{1old} – speed value at the previous iteration. For the first iteration P_{old} и ω_{old} are specified in the controller code.

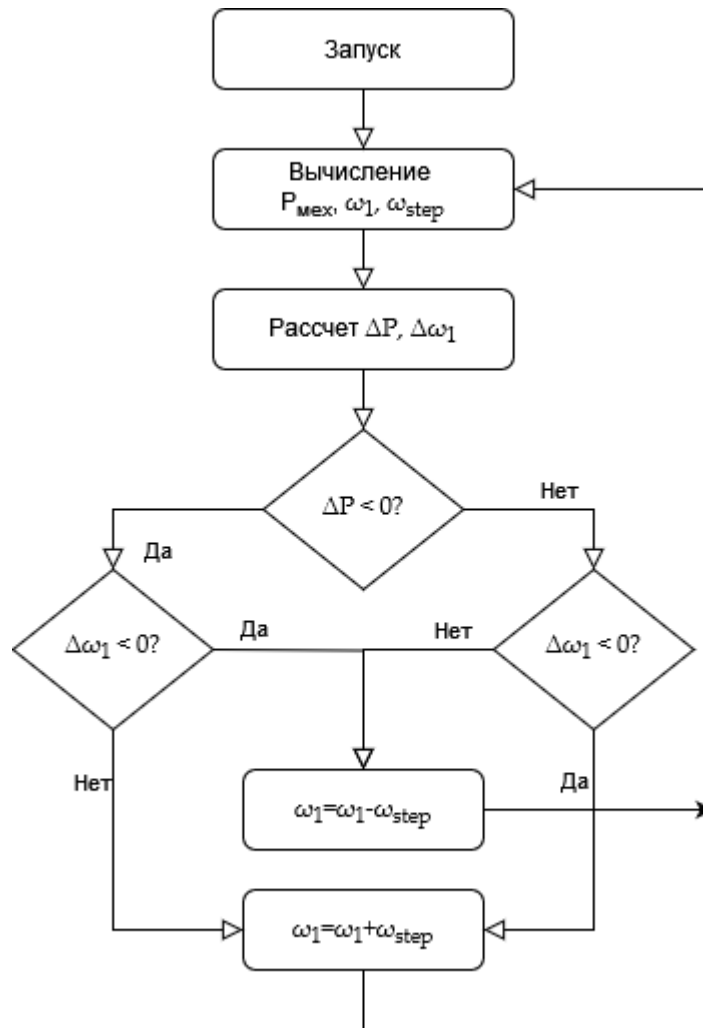


Figure 13 – Block diagram of the MPPT algorithm

4 IMPLEMENTATIONS OF THE CONTROL SYSTEM

4.1 Selection of components

To proceed to the physical embodiment of the simulated system, it is necessary to search for components.

To receive feedback on angular velocity, it is necessary to install sensors that will transmit the necessary information. It is worth considering that the cylindrical blades are in rotation relative to the central part of the wind wheel, therefore, the sensor must be non-contact. After analyzing the possible selection options, a decision was made in favor of a bipolar digital Hall sensor SS41F (Figure 14) and installation of magnets at the ends of the cylinder blades; the sensor, in turn, will be installed on the central part of the wind wheel.

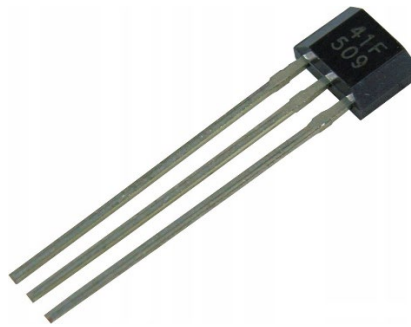


Figure 14 – Bipolar Hall sensor SS41F

The processing of the signal coming from the sensor will be performed by the Arduino Nano hardware platform with an ATmega328 microcontroller (Figure 15) instead of MyRIO. Also, the controller and all necessary calculations will be performed through the selected controller. This decision was made due to the compact form factor for convenient placement on the installation. It is worth noting that using an Arduino Nano microcontroller instead of MyRIO will allow you to significantly reduce the cost of installation, reduce energy consumption and the amount of space occupied. However, it is necessary to consider the limitations imposed by this transfer, since MyRIO has higher processing power.

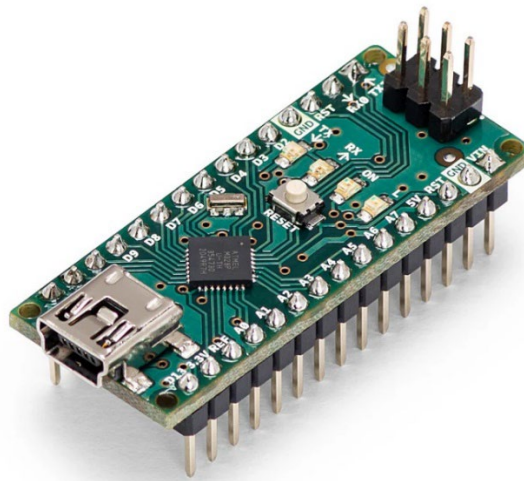


Figure 15 – Arduino Nano hardware platform

To monitor the power consumption that is supplied to the engines to start power generation, and the power output, it is necessary to install current and voltage sensors in the generator network and in the source network. To record current strength, ACS712 current sensors up to 5 and 20 amperes (Figure 16) are suitable for the generator and source, respectively, which are characterized by high accuracy and low noise levels. Inside the sensor is a Hall sensor that responds to the magnetic field created by the current passing through the conductor. The output signal of the sensor is presented in the form of an analog voltage proportional to the measured current. This simplifies the process of processing and analyzing the received data. The ACS712 has convenient microcontroller pins for easy system integration. To obtain voltage information, it was decided to use voltage dividers that will be connected to the analog ports of the controller.

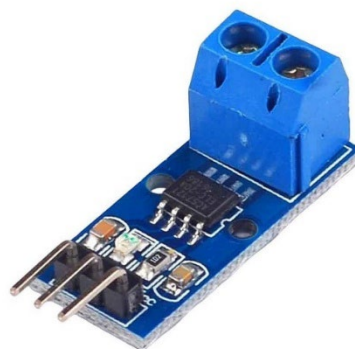


Figure 16 – ACS712 current sensor

The Arduino Uno hardware platform (Figure 17) was chosen as a controller that processes signals from current sensors and to implement the wind wheel control

algorithm based on the OTMM algorithm (Figure 17) due to its simple, intuitive interface, low cost, and extensive documentation.



Figure 17 – Arduino Uno hardware platform

The sensor installation diagram is shown in Figure 18.

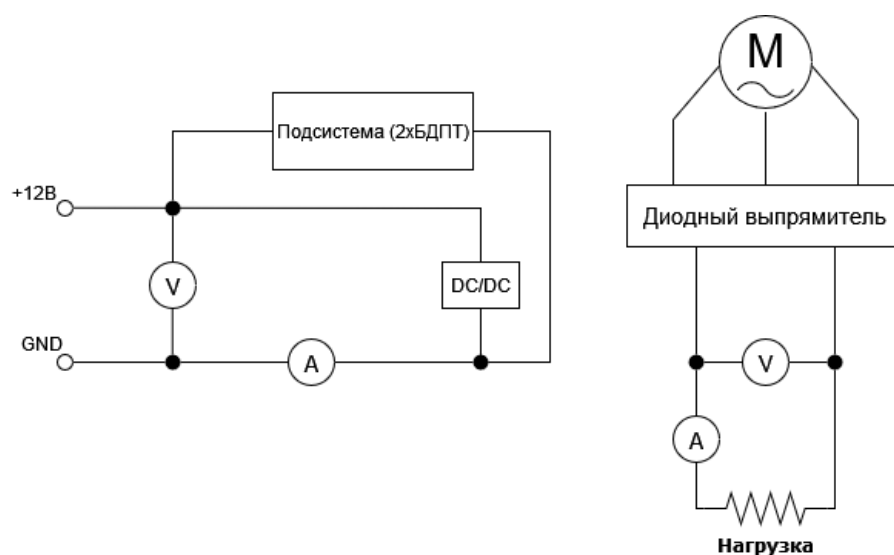


Figure 18 – Sensor layout diagram

4.2 Development of a block diagram

At the next stage, a block diagram of the system was developed, presented in Figure 19.

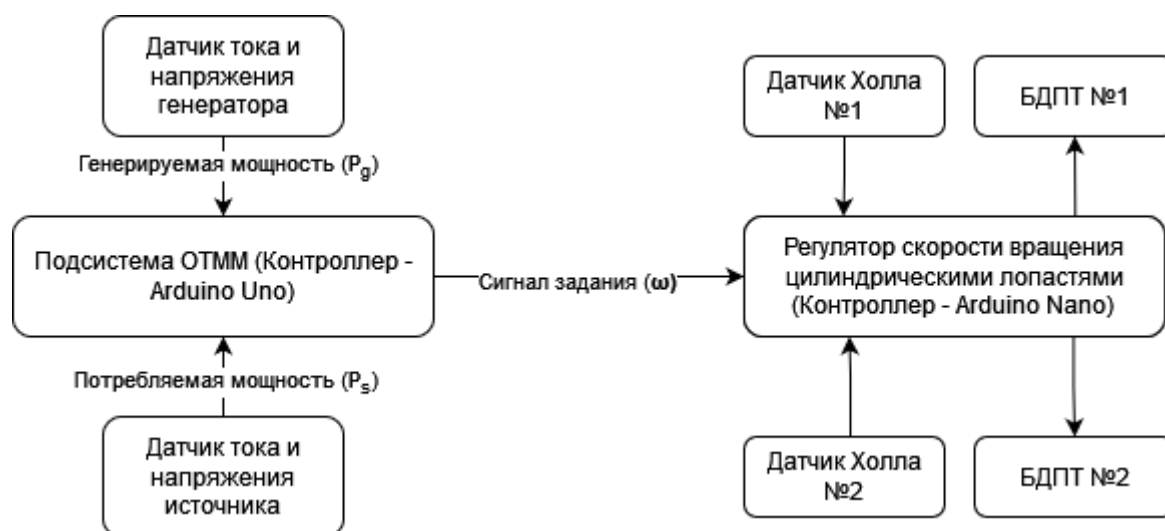


Figure 19 – System block diagram

4.3 Implementation of a cylinder control loop

To develop an operating algorithm, it is necessary to fully understand the operating principle of the Hall sensor. It consists in changing the voltage now a magnet passes through its field, which remains at a high level until the next passage of a magnet of the opposite polarity, after which the voltage decreases to a minimum. The first proposed algorithm included counting the number of revolutions over a certain time interval, after which this value was converted into rotation speed in revolutions per minute. The disadvantage of this approach was the strong dependence on the selected time interval, which led to a rough determination of the speed with large steps and, as a result, with low accuracy.

The second algorithm is based on calculating the speed after each revolution. The microcontroller calculates the time difference in milliseconds between the current and previous moments of passage of the magnet. Then, by dividing the number of milliseconds in a minute by the time value obtained because of measurements, the microcontroller determines the rotation speed in revolutions per minute. This method turned out to be more accurate.

After conducting experiments comparing speed measured manually using a hand tachometer, the discrepancy was found to be minimal within one dozen

revolutions (with speeds varying over a range of up to several thousand revolutions per minute). No false positives or omissions were detected during the experiments.

The next step is to set up the interaction between the controller and the motor driver; for this, the Arduino Servo library was used. It is worth noting that it was decided to use interrupts to read information from sensors, since interrupts allow you to instantly respond to a change in the signal from the sensor or the arrival of data via the communication interface. This provides faster, more accurate real-time processing of information and frees the processor from constantly polling the status of external devices. Instead, the processor is activated only when an event occurs (receiving a signal from a sensor), allowing it to perform the main task of regulating speed between interrupts.

It was experimentally established that when a signal other than zero is applied to the motor driver, the protective mechanism is triggered, and the engines do not start. Therefore, the first signal must always be zero. Next, the supplied signal was calibrated. First, we will need to experimentally identify the minimum signal after which the motors begin to move, after which we will determine the signal at which the motor reaches its rated speed. To do this, we will remove 20 points, from zero to one hundred degrees of the potentiometer; a graph of the dependence of angular velocity on the angle of the potentiometer is presented in Figure 20.

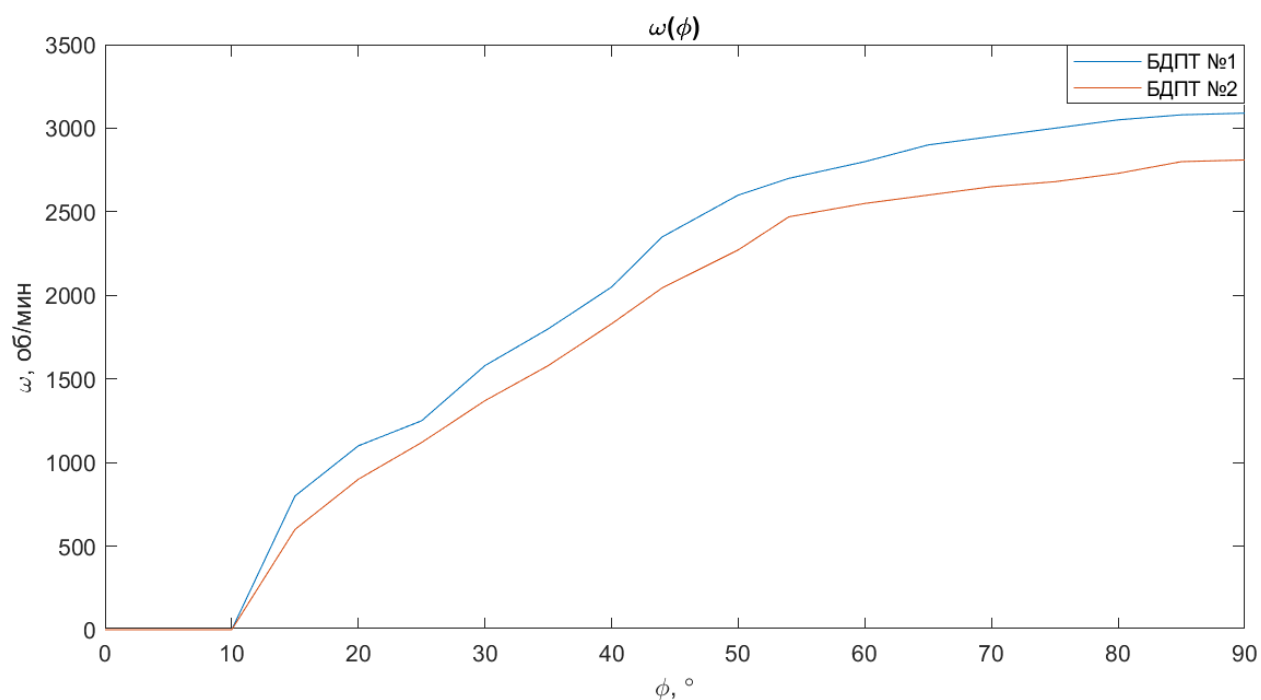


Figure 20 – Graphs of engine speed versus reference angle

As can be seen from the experiment graphs presented above, the motors begin to move when the driving force is from 12 to 15 degrees of the potentiometer angle. It is important to note that motors behave differently with the same reference signal, therefore, they reach maximum speed with different reference signals. It was found that the characteristics have a linear behavior at speeds from 500 to 2500 rpm with a reference influence of 45 and 55 degrees for the first and second engine, respectively. Further, the characteristic has a hyperbolic form, and a large step of the task causes a small increase in speed. In this connection, it was decided to choose the operating speed section where the engines behave linearly. Also, the heterogeneity of engine behavior was considered when adjusting the controller coefficients.

A complete listing of the controller algorithm code, interaction with motor drivers, speed processing and data transmission is presented in Appendix 3.

4.4 Board development and installation into the system

Next, an electrical circuit with a microcontroller was developed to which the sensors would be connected. To do this, all the necessary components were located on the board, including a microcontroller, pull-up resistors for Hall sensors, a capacitor for voltage stabilization, contacts for ease of connection, and contacts for connecting external devices for interaction via the UART interface were also considered. After this, installation work was carried out to unsolder the components on the board.

To ensure stable placement of the board and protection from installation vibrations and environmental influences, the case and mounting equipment were modeled in the SolidWorks environment, followed by printing using 3D printing technology. The model and installation results are presented in Figures 21 and 22, respectively.

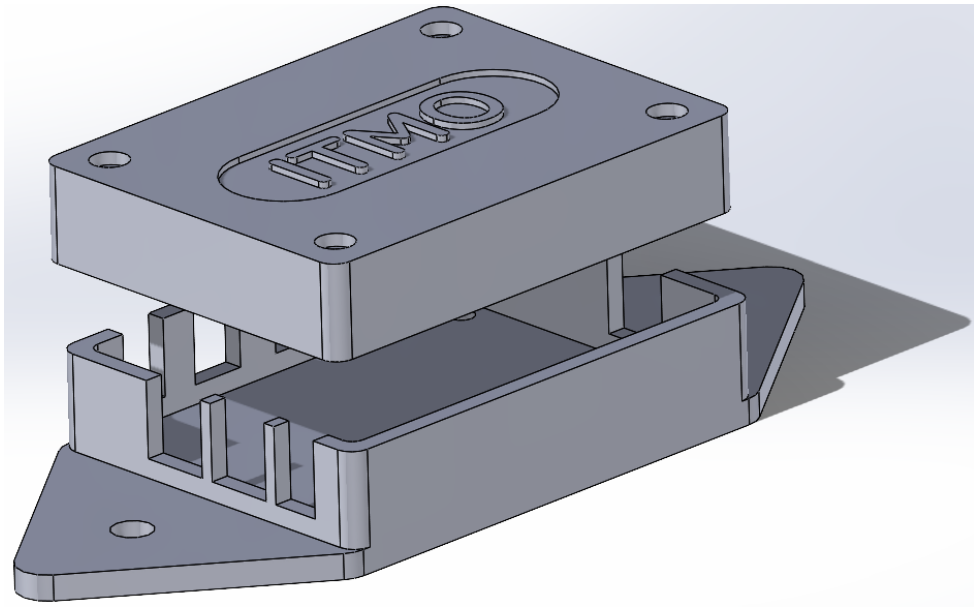


Figure 21 – Case model with fasteners in the SolidWorks environment



a)



b)

Figure 22 – Installation appearance

4.5 Experimental comparison of a real system with a model

Experiment graphs comparing the mathematical model with a real system during a jump in the driving force are presented in Figure 23.

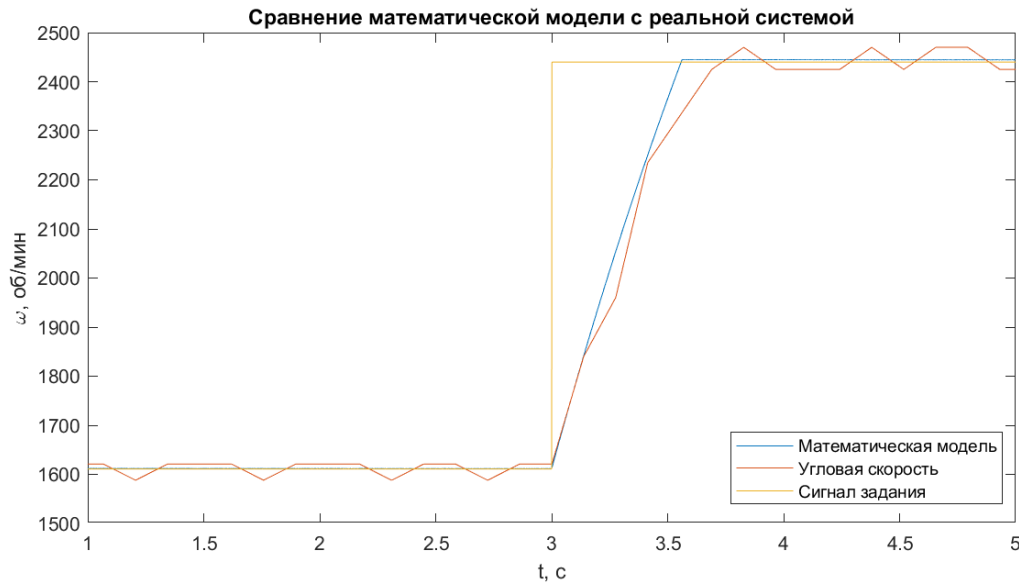


Figure 23 – System operation schedule

Transition process time of the mathematical model (5% zone):

$$\tau_M = 3.47 \text{ s} - 3 \text{ s} = 0.47 \text{ s} \quad (2.1)$$

Overshooting:

$$\sigma = \frac{2444 - 2440}{2440} = 0.16\% \quad (2.2)$$

Transition process time of the real system (5% zone):

$$\tau_p = 3.69 \text{ s} - 3 \text{ s} = 0.69 \text{ s} \quad (2.3)$$

Overshooting:

$$\sigma = \frac{2470 - 2440}{2440} = 1.2\% \quad (2.4)$$

The transient time of the real system is close to the transient time of the mathematical model, while the overshoot differs several times. This can be attributed to the fact that the sensors have a measurement error of the order of several tens of revolutions per minute. Nevertheless, the results obtained correspond to the stated requirements, therefore, we can conclude that the developments were successful.

4.6 Implementation of the wind turbine power control loop

To obtain information about the voltage, it is necessary to calculate the voltage dividers, which will send a signal to the Arduino Uno pins in proportion to the measured voltage. It was taken into account that the source voltage is constant and equal to $V_1 = 12 \text{ V}$, but the voltage taken from the generator is not constant and

varies up to 80 V, you also need to take into account that there may be surges that are undesirable for the controller, since the contacts are designed to receive a signal up to 5 V, so let $V_2 = 120$ V. Next, you need to make a calculation resistors and scaling functions for the controller, the divider circuit is shown in Figure 24. The maximum voltage that will be supplied to the controller:

$$\frac{V}{R_1 + R_2} * R_2 \quad (3.1)$$

Resistors are selected for uninterrupted operation of the system. Let for the power source:

$$R_1 = 30 \text{ k}\Omega, R_2 = 7,5 \text{ k}\Omega$$

Then:

$$\frac{12 \text{ V}}{30 \text{ k}\Omega + 7,5 \text{ k}\Omega} * 7,5 \text{ k}\Omega = 2,4 \text{ V} \quad (3.2)$$

The analog ports of the controller produce values from 0 to 1023, therefore it is necessary to scale the signal from 0 to 491.5.

Similarly, calculations were carried out for the generator:

$$R_1 = 390 \text{ k}\Omega, R_2 = 13 \text{ k}\Omega$$

$$\frac{120 \text{ V}}{403 \text{ k}\Omega} * 13 \text{ k}\Omega = 3,9 \text{ V} \quad (3.3)$$

$$3,9 \text{ V} * \frac{1024}{31} = 120$$

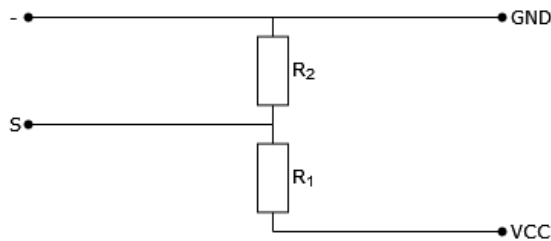


Figure 24 – Voltage divider circuit

The connection diagram of all elements of the system is shown in Figure 25. It is important to clarify that the diagram shows only one pair of current and voltage sensors for the generator, which are connected to analog pins A1 and A2 of the

Arduino Uno controller. But in a real system, a pair of current and voltage sensors for the power supply is also connected in a similar way to analog pins A3 and A4, respectively.

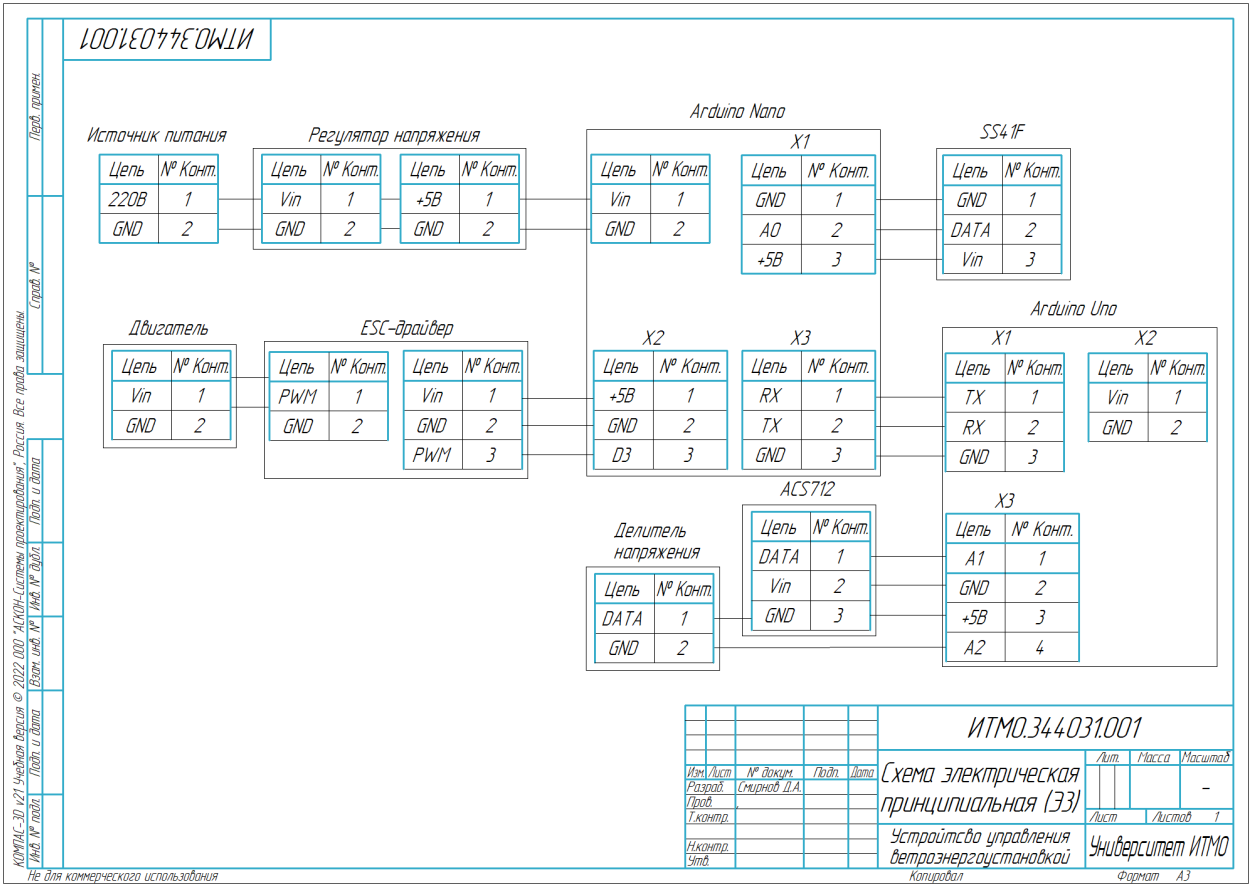


Figure 25 – Electrical connection diagram

After installing the sensors in the system, the OTMM algorithm was implemented based on the controller, which searches for the point of maximum power and remembers the value of the rotation speed of the cylindrical blades at this point, which is transmitted to the first controller to the speed control loop in the form of a task signal using the UART interface. This is a standard hardware interface that is used to transfer serial data between devices. It operates asynchronously, meaning that the transmitted data bits have no external synchronization. A complete listing of the OTMM regulator code is presented in Appendix I.

The appearance of the stand is shown in Figure 26.

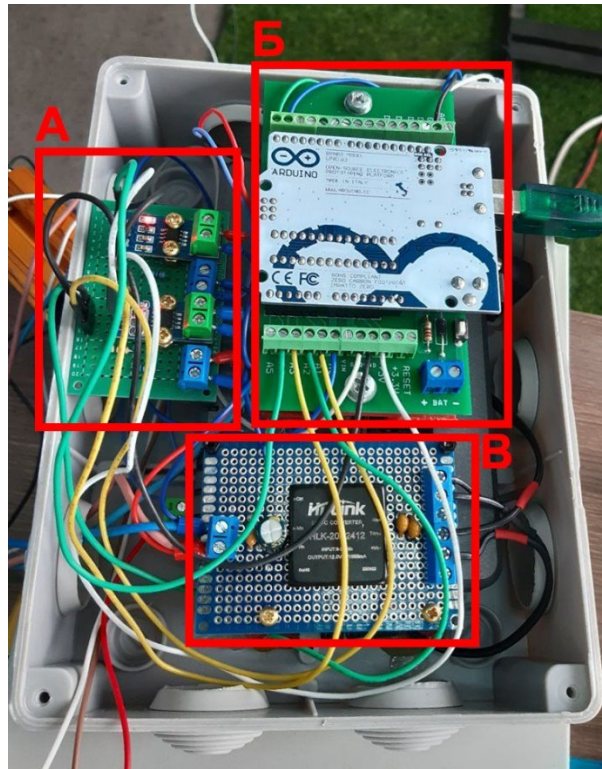


Figure 26 – Appearance of the experimental stand (A – board with sensors, B – Arduino Uno, C – voltage rectifier)

This implementation allows you to record data from all sensors, as well as the speed of rotation of the wind wheel. This will be useful for conducting experiments to confirm the operation of the algorithm.

4.7 Verification of the algorithm's operation

To test the performance of the developed system, it was decided to conduct experiments in laboratory conditions; for this purpose, an industrial fan with a large radius of wind flow was located opposite the installation, for which wind speeds were measured at different points using a hand-held anemometer, the appearance of the experimental installation with numbered points is presented in Figure 27, the measurement results are presented in Table 3. From which the fan does not act over the entire area of the wind wheel, covering approximately 40% of its diameter and blowing only one blade at a time. The average wind speed in the affected area is approximately 3–4 m/s.

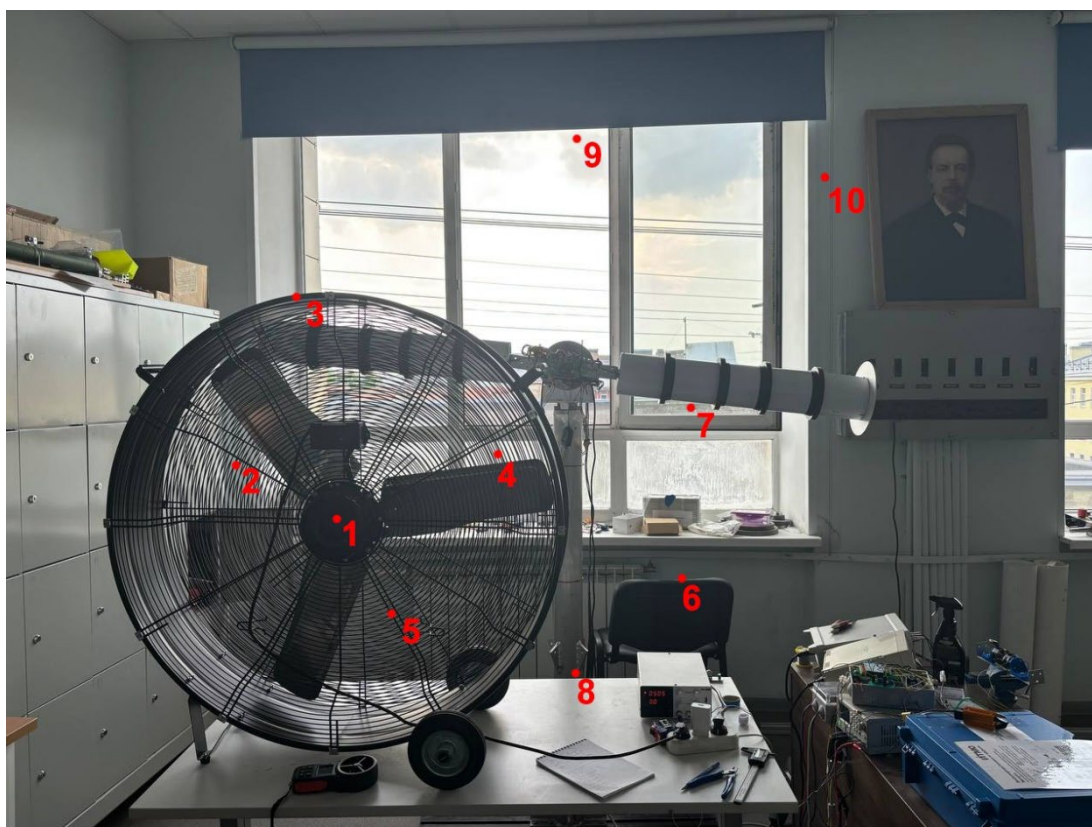


Figure 27 – Experimental setup

Table 3 – Result of wind speed measurements

Point №	Wind speed, m/s
1	1,68
2	4
3	4,5
4	4
5	4
6	1
7	1
8	2
9	0,7
10	1

Then measurements were taken under the described conditions. The energy generation graph is presented in Figure 28. From it you can see that energy generation occurs in spurts, which is logical for current conditions. This means that

the results can be increased several times to get closer to real conditions.

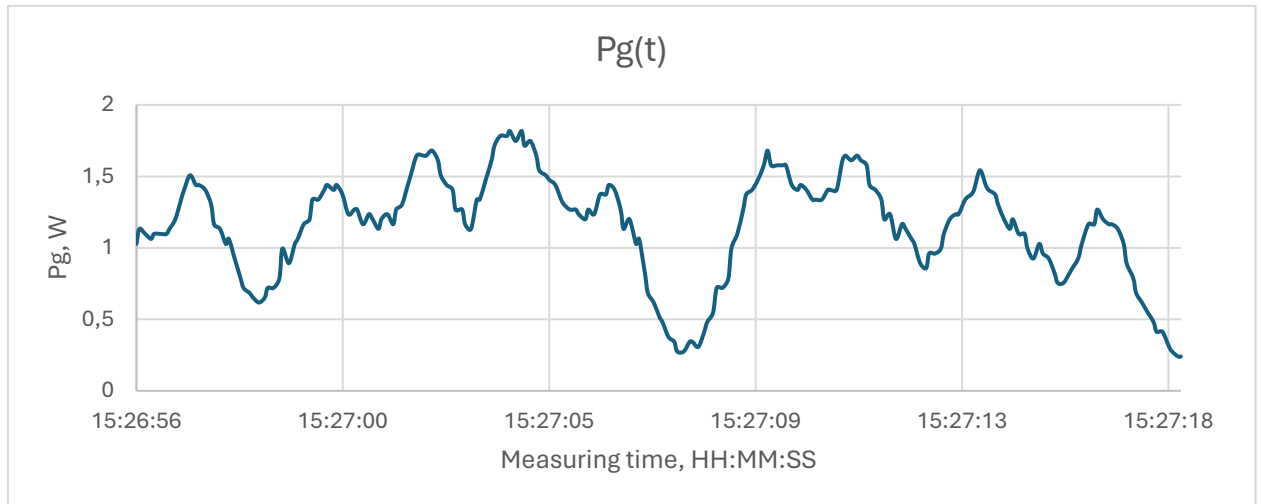


Figure 28 – Results of energy generation at constant speed

Since we cannot yet carry out experiments on the street under real conditions, to test the performance of the algorithm, it was decided to add an operational amplifier to the signal circuit of the generator sensors, which should simulate signal amplification. In this case, the algorithm functions correctly, calculating the power at each step, and then increasing the rotation speed. The results of measurements of the generated power are presented in Figure 29. The graph shows that the generated power reaches its maximum at a rotation speed of 2000–2100 rpm, where the inflection point is visible. After which, increasing the speed becomes ineffective, since the amount of energy consumed increases, and generation grows minimally, therefore the difference between the generated and consumed energy decreases.

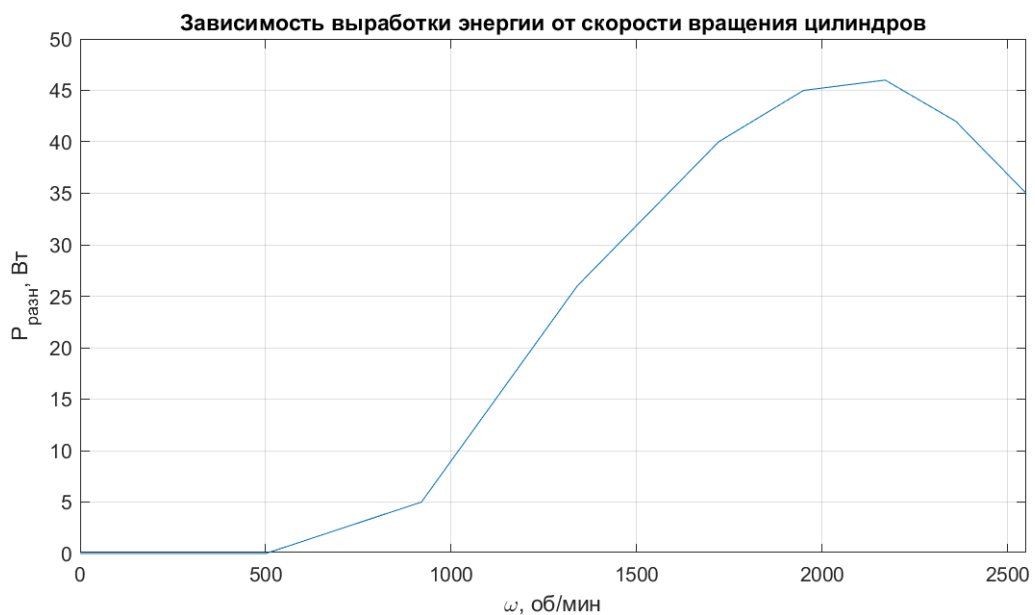


Figure 29 – Algorithm operation graph

In this case, the algorithm shows its efficiency and maintains the speed at the point of maximum power, which indicates its efficiency.

To further improve the wind power plant control system, it seems appropriate to conduct additional experiments under real weather conditions. Also, one of the promising modifications is the installation of an anemometer in the control system, which will measure wind speed and transmit the received data to the controller in real time. This will allow the maximum power point tracking (MPPT) algorithm to be modified to adapt it to changing wind conditions. The introduction of an anemometer into the control system will provide more accurate and efficient adjustment of the rotation speed of the cylindrical blades, which will increase the overall efficiency of the installation. These measures will make it possible to use available resources and increase the reliability of the entire system under various operating conditions more efficiently.

CONCLUSION

In the final qualifying work, the assigned tasks were solved to study the parameters of a wind power plant based on the Magnus effect and a control system was developed and implemented with an operating mode at the operating point with the maximum generated power. During work:

- a mathematical model of the electric drive system of a rotating cylindrical wind wheel blade has been developed, based on the parameters of the element base and experimental studies of engine characteristics;
- a system for controlling the rotation speed of a cylindrical wind wheel blade was developed, which was implemented on the basis of an Arduino Nano controller and an SS41F encoder;
- a comparison of the results of a model and experimental study of the electric drive system of a rotating cylindrical wind wheel blade with the proposed closed-loop rotation speed control system was carried out, confirming the functionality of the developed control system. Experiments for the control loop for the speed of rotation of cylindrical blades showed that the transient process time for the real system was 0.69 seconds, and for the mathematical model - 0.47 seconds. Overshoot in the mathematical model was 0.16%, in the real system - 1.2%. These indicators correspond to the stated technical requirements and indicate the correct operation of the system;
- measuring stages have been developed for feedback loops necessary to implement the algorithm for searching and tracking the maximum power point, including current sensors based on the ACS712 microcircuit and voltage sensors for the internal consumption source and generator;
- a design solution for installation and connection diagrams of current and voltage sensors to an existing wind power plant have been developed;
- a control algorithm has been developed that implements the search for the maximum power point, implemented on the basis of the Arduino Uno controller. Since in laboratory tests using an industrial fan it is impossible to create the wind flow necessary for a positive energy balance of the system, a hardware generation simulator was used to test the performance of the algorithm;

- recommendations were developed for further improvement of the wind power plant.

REFERENCES

1. Marzuki, Mohd Rafie, Romli, Ahmad, and Abdul Hamid. An overview of horizontal-axis Magnus wind turbines. – 2018 – URL: <https://iopscience.iop.org/article/10.1088/1757-899X/405/1/012011/pdf>
2. Bychkov N M, Dovgal A V, Kozlov V V. Magnus wind turbines as an alternative to the blade ones. J. Phys. Conf. Ser. 2007; 75: 12004
3. Jinbo M, Ceretta Moreira M, Lellis Hoss D, Farret F A, Cardoso Junior G. Fixed and adaptive step HCC algorithms for MPPT of the cylinders of Magnus wind turbines. 3rd Renewable Power Generation Conference. – 2014 – URL: https://www.researchgate.net/publication/283042642_MPPT_of_Magnus_Wind_System_with_DC_Servo_Drive_for_the_Cylinders_and_Boost_Converter
4. Egemen Ol Ogretim, Durmus Uygun, Mehtap Ozdemir Koklu. Analytical Evaluation of Solar Enhanced Magnus Effect Wind Turbine Concept. – 2016 – URL: https://www.researchgate.net/publication/307934726_Analytical_Evaluation_of_Solar_Enhanced_Magnus_Effect_Wind_Turbine_Concept
5. Challenergy Inc. Next generation wind turbine that harnesses energy from typhoon. – 2023 – URL: <http://copjapan.env.go.jp/cop/cop24/en/pavilion/04/>
6. Ayerolla ООО, Минск. Ветрогенераторы с эффектом Магнуса. – 2015 – URL: <https://infotechnic.pro/vetrogeneratory-s-effektom-magnusa/>
7. Институт теоретической и прикладной механики имени С. А. Христиановича СО РАН, Новосибирск. Ветроустановка с эффектом Магнуса. – 2015 – URL: http://www.itam.nsc.ru/technologies/designs/lab8/vetroustanovka_s_effektom_magnusa_lab_8.html
8. Шутов А. Д., Попов А. И. Уральский федеральный университет. ВЭУ с использованием эффекта Магнуса. – 2015 – URL: https://elar.urfu.ru/bitstream/10995/88821/1/eir_2014_2_114.pdf
9. A. Lukin, G. Demidova, D. Lukichev, N. Poliakov, A. Anuchin. Optimization of Cylindrical Blades for Wind Turbine Based on Magnus Effect – 2023 – URL: <https://ieeexplore.ieee.org/document/10290749>

Appendix A

T-Motor MN4014-9 KV400 brushless DC motor. Datasheet:
store.tmotor.com/mn4014-kv400-motor-navigator-type.html

Specifications:

Internal resistance: 67 mOhm

Shaft diameter: 4 mm

Stator diameter: 40 mm

Weight: 150 g

Maximum power 900 W

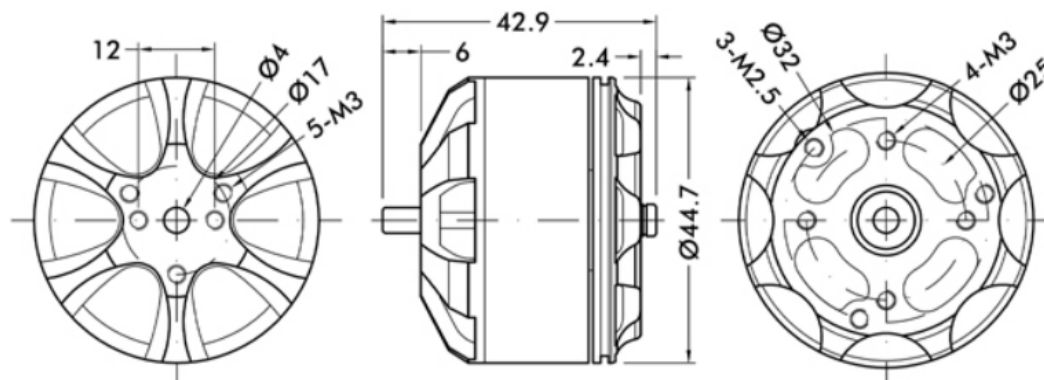
Maximum current: 30A

No-load current: 1.3 A

Engine size: $\Phi 44.7 \times 34.5$ mm

Engine

drawing:



Appendix B

ESC driver (electronic speed controller) Hobbywing Skywalker HW-BQ8009 80A-UBEC. Datasheet: <http://www.hobbywingdirect.com/skywalker-esc>

Specifications:

Constant current: 80A

Maximum current: 100A

Weight: 79 g

Dimensions: 85x36x9

Input pins: 12AWG

Output Contacts: 14AWG

Input voltage: 3-6V

Appendix C

Field effect transistor TPCA8057-H. Datasheet:

https://toshiba.semicon-storage.com/TPCA8057-H_datasheet

Specifications:

Ron FET Resistance (Ohm): $6.25 \cdot 10^{-4}$

Internal diode inductance Lon (H): 0

Diode internal resistance Rd (Ohm): $4.67 \cdot 10^{-4}$

Internal diode forward voltage Cf (V): 0.75

Damping resistance Rs (Ohm): $1 \cdot 10^6$

Damping capacitance Cs (uF): 0.33

Appendix D

Hall sensor bipolar digital SS41F. Datasheet:

<https://static.chipdip.ru/lib/048/DOC013048609.pdf>

Specifications:

Mounting type: through hole

Output voltage: 0.4V

Maximum operating temperature: +150 C

Maximum output current: 20mA

Minimum operating temperature: -40 C

Supply voltage – max.: 24 V

Supply voltage - min.: 4.5 V

Operating supply voltage: 24 V

Power supply operating current: 10A

Type: Bipolar Hall Sensor with Latch

Weight, g: 0.14

Appendix E

Arduino Nano hardware platform. Datasheet: [arduino.cc/hardware/nano/](https://www.arduino.cc/hardware/nano/)

Specifications:

Microcontroller: Atmel ATmega328

Architecture: AVR

Operating voltage: 5V

Flash memory: 32 KB, of which 2 KB is used by the bootloader

Clock frequency: 16 MHz

Analogue inputs: 8

Input voltage: 7-12V

Digital inputs: 22 (6 of which are ADC)

ADC outputs: 6

Weight: 7 g

Appendix F

Current sensor ACS712 5A/20A. Datasheet: static.chipdip.ru/lib/837.pdf

Specifications:

Bandwidth: 80 kHz

Total output error: 1.5% at $T_A = 25^{\circ}\text{C}$

Internal conductor resistance: 1.2 mOhm

Supply voltage: 5V, single-supply mode

Output sensitivity: 66 to 185 mV/A.

Appendix G

Arduino Uno hardware platform. Datasheet: arduino.cc/uno/datasheet

Specifications:

Microcontroller: Atmel ATmega328P

Operating voltage: 5V

Input voltage: 7-12V

Input voltage limit: 6–20 V

Digital inputs: 14 (6 of which are ADC)

ADC outputs: 6

Analogue inputs: 6

Flash memory: 32 KB, of which 0.5 KB is used by the bootloader

Clock frequency: 16 MHz

Length: 68.6 mm

Width: 53.4 mm

Weight: 25 g

Appendix H

Source code listing for the cylindrical blade speed controller in C++ (Arduino):

```
#include <Servo.h>
#include <Streaming.h>

// Max velocity of 1st engine - 2800 (100 degrees)
// Max velocity of 2nd engine - 2800 (110 degrees)

Servo ESC1; // 1st engine (Right)
Servo ESC2; // 2nd engine (Left)

const int sensorPin1 = 2; // 1st Hall effect sensor with interruption
const int sensorPin2 = 3; // 2nd Hall effect sensor with interruption

int sensorPin3 = A2; // Pin for reference signal #1
int sensorPin4 = A3; // Pin for reference signal #2

int sensorValueRef = 0; // Reference signal for 1st engine from 0 to 1023

int referenceValue1 = 0; // Mapped 1st reference signal in degrees (0-100)
int referenceValue2 = 0; // Mapped 2nd reference signal in degrees (0-110)

int referenceValueRPM1 = 0; // Mapped 1st reference signal in rpm (0-2800)
int referenceValueRPM2 = 0; // Mapped 2nd reference signal in rpm (0-2800)

volatile int velocity1 = 0; // 1st engine measured velocity
volatile int velocity2 = 0; // 2nd engine measured velocity

volatile unsigned long timeOfLastCrossing1 = 0; // Crossing of magnet for 1st
sensor
volatile unsigned long timeOfLastCrossing2 = 0; // Crossing of magnet for 2nd
sensor

float eintegral1 = 0;
float eintegral2 = 0;

float deltaT = 0.01;

void setup() {
    Serial.begin(9600);

    // Pins defining for engines
    ESC1.attach(5, 1000, 2000);
    ESC2.attach(6, 1000, 2000);

    // Velocity measuring using interruptions
    attachInterrupt(digitalPinToInterrupt(sensorPin1), calcVelocity1, FALLING);
    attachInterrupt(digitalPinToInterrupt(sensorPin2), calcVelocity2, FALLING);
}
```

```

void loop() {
    sensorValueRef = analogRead(sensorPin3);

    referenceValue1 = map(sensorValueRef, 0, 1024, 0, 45);
    referenceValue2 = map(sensorValueRef, 0, 1024, 0, 55);

    referenceValueRPM1 = map(referenceValue1, 0, 45, 0, 2500);
    referenceValueRPM2 = map(referenceValue2, 0, 55, 0, 2500);

    // Computing of the control signal u
    float kp1 = 16;
    float ki1 = 2;
    float kp2 = 13;
    float ki2 = 1.8;

    float e1 = referenceValueRPM1 - velocity1;
    float e2 = referenceValueRPM2 - velocity2;
    eintegrall1 = eintegrall1 + e1 * deltaT;
    eintegral2 = eintegral2 + e2 * deltaT;

    float u1 = kp1 * e1 + ki1 * eintegrall1;
    float u2 = kp2 * e2 + ki2 * eintegral2;

    // Set the motor speed
    float pwrfl = map(u1, 0, 2444, 0, 45);
    float pwr2 = map(u2, 0, 2454, 0, 55);
    int pwr1 = (int) pwrfl;
    int pwr2 = (int) pwr2;

    // Artificial limitation
    if (pwr1 > 47) {
        pwr1 = 47;
    }
    if (pwr2 > 56) {
        pwr2 = 56;
    }

    ESC1.write(pwr1);
    ESC2.write(pwr2);

    if (millis() - timeOfLastCrossing1 > 900) velocity1 = 0;
    if (millis() - timeOfLastCrossing2 > 900) velocity2 = 0;

    Serial << "1st: refValue: " << referenceValue1 << "; refValueRPM: " <<
referenceValueRPM1 << "; Real velocity: " << velocity1 << "| 2nd: " <<
referenceValue2 << "; refValueRPM: " << referenceValueRPM2 << "; Real
velocity: " << velocity2 << endl; // Results printing
}

```

```
void calcVelocity1() {  
    unsigned long currentTime = millis();  
    unsigned long rotationTime = currentTime - timeOfLastCrossing1;  
    velocity1 = 60000 / rotationTime;  
    timeOfLastCrossing1 = currentTime;  
}  
  
void calcVelocity2() {  
    unsigned long currentTime = millis();  
    unsigned long rotationTime = currentTime - timeOfLastCrossing2;  
    velocity2 = 60000 / rotationTime;  
    timeOfLastCrossing2 = currentTime;  
}
```

Appendix I

Listing of the source code of the wind wheel power controller (MPPT) in C++ (Arduino):

```
#define PIN_OUTSV A1
#define PIN_OUTGV A2
#define PIN_OUTSC A3
#define PIN_OUTGC A4

ACS712 dataI1(PIN_OUTSC);
ACS712 dataI2(PIN_OUTGC);

float sourceCurrent = 0;
float sourceVoltage = 0;
float generatorCurrent = 0;
float generatorVoltage = 0;
float Ps = 0;
float Pg = 0;
float Pold = -100;
int velRef = 300;
int velStep = 50;

void setup() {
    Serial.begin(9600);
    delay(5000);
}

void loop() {
    sourceVoltage = mapfloat(analogRead(PIN_OUTSV), 0, 491.52, 0, 12);
    generatorVoltage = mapfloat(analogRead(PIN_OUTGV), 0, 875, 0, 120);
    sourceCurrent = mapfloat(analogRead(PIN_OUTSC), 0, 1024, -20, 20);
    generatorCurrent = mapfloat(analogRead(PIN_OUTGC), 0, 1024, -5, 5);
    Ps = sourceVoltage * sourceCurrent;
    Pg = - generatorVoltage * generatorCurrent;

    if (Pg - Ps > Pold) {
        velRef = velRef - velStep;
    } else {
        velRef = velRef + velStep;
    }
    Pold = Pg - Ps;
    delay(3000);
}

float mapfloat(long x, long in_min, long in_max, long out_min, long out_max)
{
    return (float)(x - in_min) * (out_max - out_min) / (float)(in_max - in_min)
    + out_min;
}
```